



Audio Engineering Society

Convention Paper 7901

Presented at the 127th Convention
2009 October 9–12 New York, NY, USA

The papers at this Convention have been selected on the basis of a submitted abstract and extended precis that have been peer reviewed by at least two qualified anonymous reviewers. This convention paper has been reproduced from the author's advance manuscript, without editing, corrections, or consideration by the Review Board. The AES takes no responsibility for the contents. Additional papers may be obtained by sending request and remittance to Audio Engineering Society, 60 East 42nd Street, New York, New York 10165-2520, USA; also see www.aes.org. All rights reserved. Reproduction of this paper, or any portion thereof, is not permitted without direct permission from the Journal of the Audio Engineering Society.

Visualization and analysis tools for low frequency propagation in a generalized 3D acoustic space

Adam J. Hill¹ and Malcolm O. J. Hawksford²

¹ ajhilla@essex.ac.uk ² mjh@essex.ac.uk

Audio Research Laboratory, School of Computer Science and Electronic Engineering,
University of Essex, Colchester, UK CO4 3SQ

ABSTRACT

A toolbox is described that enables 3D animated visualization and analysis of low-frequency wave propagation within a generalized acoustic environment. The core computation exploits a Finite-Difference Time-Domain (FDTD) algorithm selected because of its known low frequency accuracy. Multiple sources can be configured and analyses performed at user-selected measurement locations. Arbitrary excitation sequences enable virtual measurements embracing both time-domain and spatio-frequency domain analysis. Examples are presented for a variety of low-frequency loudspeaker placements and room geometries to illustrate the versatility of the toolbox as an acoustics design aid.

1. INTRODUCTION

When dealing with problematic room acoustics, a tool that provides in-depth visualization and analysis options for wave propagation and interaction can be highly useful. Tools of this variety have been previously developed, but don't tend to focus on low frequency behavior.

Most existing acoustical design tools operate using image source or ray tracing simulation methods [1-3]. While these techniques can provide very accurate results at higher frequencies, they tend to become inaccurate as wavelengths approach and surpass the dimensions of a room. The Finite-Difference Time-

Domain (FDTD) simulation method is well known in electromagnetics and has been steadily gaining popularity in acoustics. FDTD can provide extremely accurate modeling of low frequencies and has been utilized often in recent acoustics simulation research [4-7].

The toolbox presented in this paper takes previous work with FDTD and acoustical analysis and ties them together into an easy to use package that allows for maximum control of the acoustical and electrical environments. It was developed to focus on the control of low frequency behavior in listening rooms where room modes can cause widely varying listening experiences across a space.

2. FINITE-DIFFERENCE TIME-DOMAIN SIMULATION METHOD

The Finite-Difference Time-Domain (FDTD) simulation method operates by making the sound wave equation discrete in both the temporal and spatial frequency domains. The resulting set of partial differential equations governs the simulation which operates in a leap-frog scheme, alternating between sound pressure and particle velocity updates, which is laid out in a staggered grid (Figure 1).

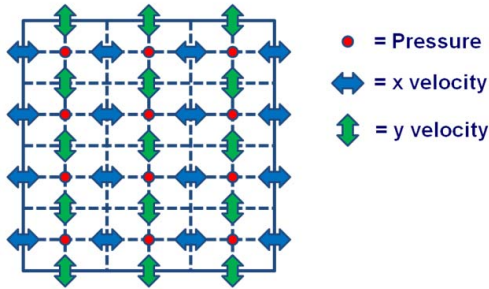


Figure 1: FDTD simulation spatial layout

All sound pressure and particle velocity values in the FDTD grids are initialized to zero with one (or more) pressure point selected as the source location. The source location will eventually produce a non-zero pressure value that will then be used to update the surrounding particle velocity points. Every adjacent point has an effect on the point being updated. Key equations involved in this process are as follows (adapted from [4]):

$$u^x_{x+\frac{dx}{2},y,z}\left(t+\frac{dt}{2}\right)=u^x_{x+\frac{dx}{2},y,z}\left(t-\frac{dt}{2}\right)-\frac{dt}{\rho dx}\left[p_{x+dx,y,z}(t)-p_{x,y,z}(t)\right] \quad (1)$$

$$u^y_{x,y+\frac{dy}{2},z}\left(t+\frac{dt}{2}\right)=u^y_{x,y+\frac{dy}{2},z}\left(t-\frac{dt}{2}\right)-\frac{dt}{\rho dy}\left[p_{x,y+dy,z}(t)-p_{x,y,z}(t)\right] \quad (2)$$

$$u^z_{x,y,z+\frac{dz}{2}}\left(t+\frac{dt}{2}\right)=u^z_{x,y,z+\frac{dz}{2}}\left(t-\frac{dt}{2}\right)-\frac{dt}{\rho dz}\left[p_{x,y,z+dz}(t)-p_{x,y,z}(t)\right] \quad (3)$$

$$p_{x,y,z}(t+dt)=p_{x,y,z}(t)-\frac{c^2\rho dt}{dx}\left[u^x_{x+\frac{dx}{2},y,z}\left(t+\frac{dt}{2}\right)-u^x_{x-\frac{dx}{2},y,z}\left(t+\frac{dt}{2}\right)\right]-\frac{c^2\rho dt}{dy}\left[u^y_{x,y+\frac{dy}{2},z}\left(t+\frac{dt}{2}\right)-u^y_{x,y-\frac{dy}{2},z}\left(t+\frac{dt}{2}\right)\right]-\frac{c^2\rho dt}{dz}\left[u^z_{x,y,z+\frac{dz}{2}}\left(t+\frac{dt}{2}\right)-u^z_{x,y,z-\frac{dz}{2}}\left(t+\frac{dt}{2}\right)\right] \quad (4)$$

Where $u^x_{x,y,z}(t)$, $u^y_{x,y,z}(t)$ and $u^z_{x,y,z}(t)$ are the particle velocity components for each of the three dimensions and $p_{x,y,z}(t)$ is the sound pressure at a point specified by x, y, z and time step, t . Points are spaced according to dx, dy, dz and the simulation is updated based on the time step, dt . The speed of sound and air density are represented with c and ρ , respectively.

To ensure simulation stability, the maximum time step size can be determined by the grid spacing. This will ensure that there is no spatial or temporal aliasing during the simulation [6].

$$dt \leq \frac{1}{c\sqrt{\frac{1}{dx^2} + \frac{1}{dy^2} + \frac{1}{dz^2}}} \quad (5)$$

While equation (4) will correctly update all pressure points in the grid, equations (1-3) will not function at room boundaries. This is because the particle velocity update equations require knowledge of pressure values at surrounding grid points. At a boundary, only one pressure value is available for the calculation, therefore a special set of particle velocity boundary condition equations must be used.

The corresponding particle velocity update equation for a positive x-direction boundary occurrence is (adapted from [4]):

$$u^x_{x,y,z}\left(t+\frac{dt}{2}\right)=\frac{R_x-Z}{R_x+Z}u^x_{x,y,z}\left(t-\frac{dt}{2}\right)+\frac{2}{R_x+Z}p_{x,y,z}(t) \quad (6)$$

The characteristic wall impedance, Z , is defined by $Z=\rho c\frac{1+\sqrt{1-\alpha}}{1-\sqrt{1-\alpha}}$, where α is the boundary absorption coefficient and $R_x=\frac{\rho dx}{dt}$. Simply switching the sign in

front of the pressure component will give the update equation for a negative x-direction boundary occurrence.

$$u_{x,y,z}^x \left(t + \frac{dt}{2} \right) = \frac{R_x - Z}{R_x + Z} u_{x,y,z}^x \left(t - \frac{dt}{2} \right) - \frac{2}{R_x + Z} P_{x,y,z}(t) \quad (7)$$

Equations (6-7) can be modified to apply to the y- and z-directions. These boundary conditions are frequency independent and only concern the neighboring pressure point in the x-direction. If greater accuracy is required, these equations can be expanded to include surrounding pressure points in all directions and also frequency-dependent boundaries. This has been demonstrated by others in previously published work [8].

3. FDTD SIMULATION OF NON-RECTANGULAR SPACES

Given that FDTD operates using a collection of grids with points around edges defined as boundaries, it is not too far of a leap to expand the simulation from rectangular to non-rectangular. This can be accomplished by deriving a set of masks for the pressure and particle velocity data matrices. In this work, the pressure grid mask is first defined by the user (Figure 2). Any point in the pressure mask set to '1' indicates that point being within the simulation space. All points assigned '0' will be ignored in the simulation.

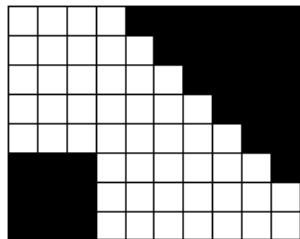


Figure 2: Two-dimensional example of a pressure grid mask (white = inside room)

Next, since particle velocity updates at boundaries require neighboring pressure points for proper calculation, masks must be generated that point to the required pressure points (Figure 3).

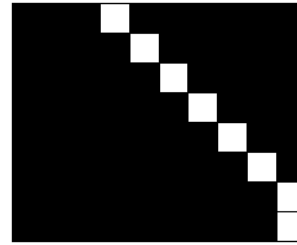


Figure 3: Pressure grid mask for positive x-direction boundary condition updates (white = inside room)

Once all the pressure point-related masks have been generated, particle velocity masks must be created. This requires some care, since all particle velocity grids are exactly one grid point larger in each dimension due to the FDTD staggered grid layout. After the initial generation of the particle velocity masks, points assigned a '1' (inside the space) that are bordered by a '0' (outside the space) will be transferred to special masks relating to boundary conditions (Figure 4).

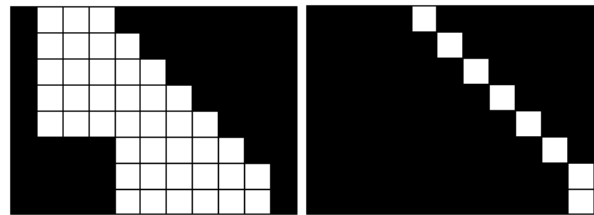


Figure 4: Two-dimensional example of particle velocity masks (left = non-boundary, right = positive x-direction boundary condition)

Again, care must be taken to properly transfer these masks between pressure and velocity grid dimensions as each type of update requires values from the other. A number of additional masks are required for proper simulation and can be easily derived directly from the above masks.

For increased accuracy it is possible to apply a finer mesh size around non-rectangular boundaries to give a smoother surface. This technique has been explained in great detail in [9] but has not yet been applied in this work.

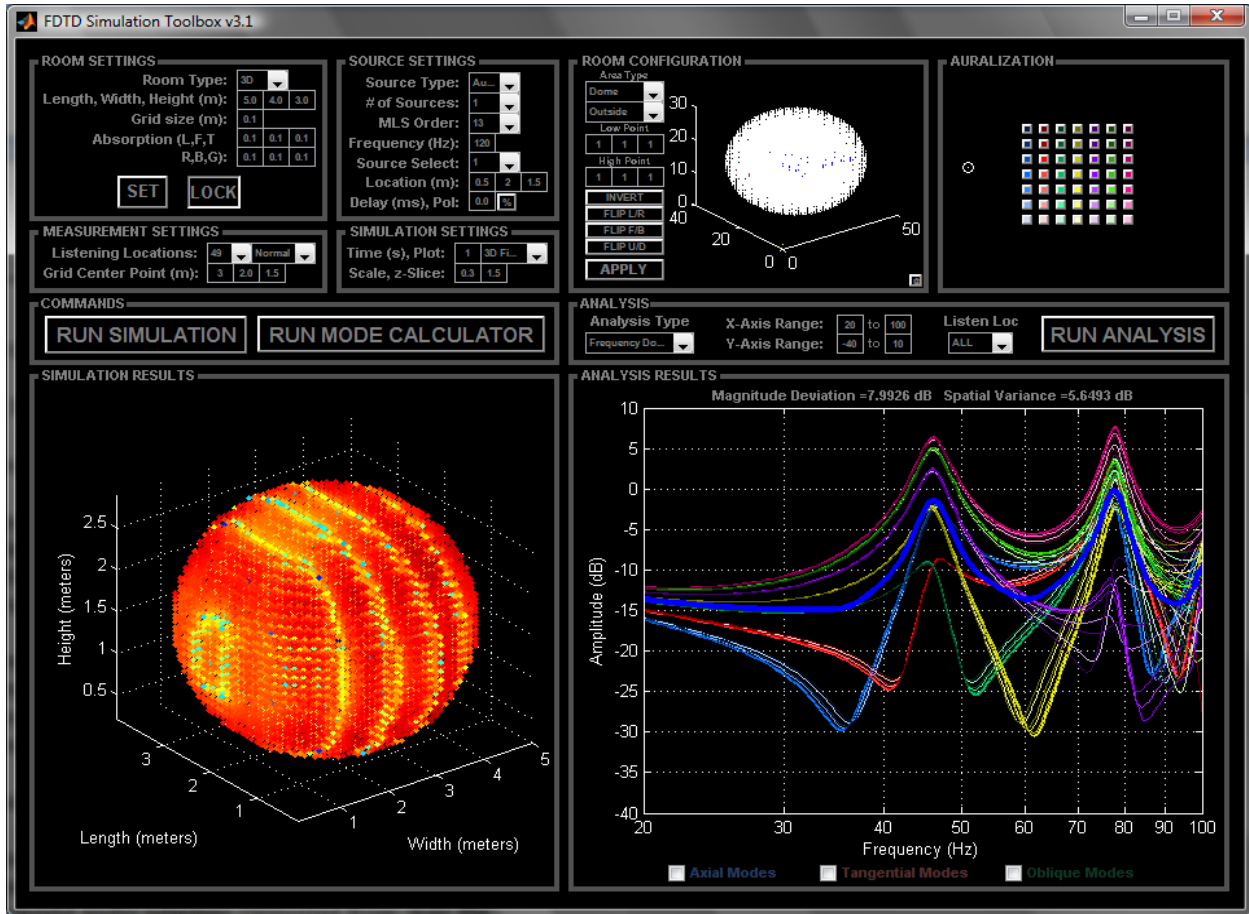


Figure 5: FDTD simulation toolbox GUI layout in Matlab

4. FDTD SIMULATION TOOLBOX

The FDTD simulation techniques described in Sections 2 and 3 have been applied to a self-contained piece of software written entirely in Matlab. This toolbox allows for simulation of a 2D or 3D space of any shape with any number of obstacles placed within. During the simulation it is possible to display animations of the pressure distribution in the space by simply plotting the sound pressure grid. Once the simulation is complete, a number of analysis options are available in addition to a simple auralization function.

The program is laid out as a user-friendly GUI where room setup, source definition, simulation, analysis and auralization can all be performed without the need to open any extra windows or programs (Figure 5).

First, the user must enter the room dimensions, grid spacing and wall absorption in the “Room Setup” area in the toolbox. From there, a visualization of the pressure point grid will appear where the user can select groups of points to add/remove from the space in the “Room Configuration” section using a cookie cutter-like approach (Figure 6). This gives the user full control over the room shape and allows for as realistic of space simulations as desired.

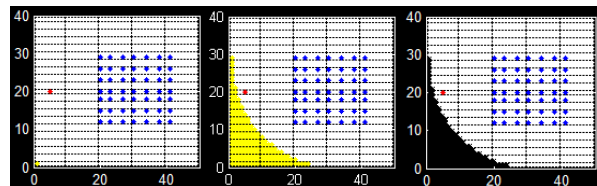


Figure 6: 2D room shaping example (left = initial room layout, center = highlighted pressure points, right = updated room layout)

After the room shape has been set, a grid of virtual listening locations can be setup in the “Measurement Settings” section where the sound pressure at each point will be recorded during simulation to be used later for analysis and auralization.

Finally, up to eight point sources can be placed within the space, driven by a range of signals including: Gaussian pulse, sinusoid, Maximum Length Sequence (MLS), tone burst, swept sinusoid and any real-world audio selection (imported from .wav file). This is all performed in the “Source Settings” section.

An additional feature built in to assist in the verification of the simulation software is a room mode calculator. This calculator operates using a simple equation based on the room’s dimensions and the speed of sound [10].

$$f = \frac{c}{2} \sqrt{\left(\frac{\eta_x}{x}\right)^2 + \left(\frac{\eta_y}{y}\right)^2 + \left(\frac{\eta_z}{z}\right)^2} \quad (8)$$

Where f is the calculated room mode (Hz) based on the room dimensions x , y and z and mode numbers η_x , η_y , and η_z . Modes with only one non-zero mode number correspond to axial modes (two surfaces involved). Two non-zero mode numbers corresponds to tangential modes (four surfaces involved) while three non-zeros mode numbers give oblique modes (six surfaces involved) [11]. This type of modal calculation is only valid for three-dimensional rectangular rooms. It assumes the room is constructed of three sets of parallel surfaces.

The room mode calculator operation displays two plots of expected modal behavior. First, a modal distribution versus frequency plot is displayed (Figure 7) and then the user is able to investigate the spatial distribution of a given room mode in the secondary plot (Figures 8-10).

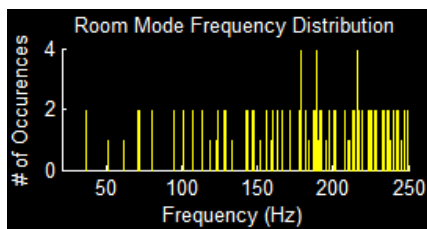


Figure 7: Frequency distribution of room modes for a 5 x 5 x 3 m room (calculated up to 250 Hz)

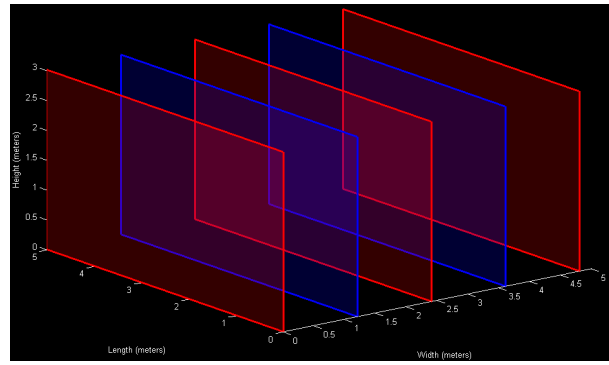


Figure 8: Spatial distribution of an axial mode (71.5 Hz) in a 5 x 5 x 3 m room (red = antinode, blue = node)

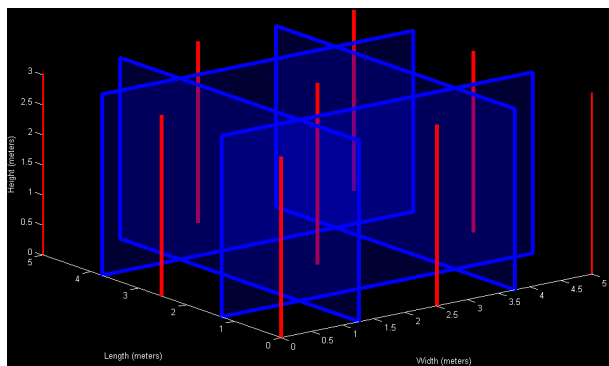


Figure 9: Spatial distribution of a tangential mode (101 Hz) in a 5 x 5 x 3 m room (red = antinode, blue = node)

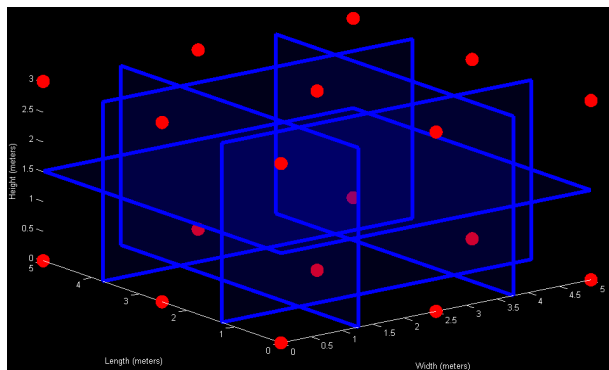


Figure 10: Spatial distribution of an oblique mode (118 Hz) in a 5 x 5 x 3 m room (red = antinode, blue = node)

Once the simulation has completed, these expected modal values can be compared to the frequency response measured at the virtual listening locations. In addition to frequency response, the “Analysis Results” section of the program allows for examination of room

layout, time domain, spectrogram and input versus output comparisons in the frequency domain.

The frequency domain analysis uses two metrics to measure how the room acoustics affect the listening experience. These two metrics are called magnitude deviation and average spatial variance. Magnitude deviation calculates the frequency response's deviation from "flat" (0 dB) at each measurement location and averages the calculated values to give a single value. The closer the magnitude deviation is to 0 dB, the flatter the frequency response of the room [12].

$$MD = \sqrt{\frac{1}{n_f - 1} \sum_{i=f_{low}}^{f_{high}} (x_i - \bar{x})^2} \quad (9)$$

Where the magnitude deviation, MD , is calculated over the frequency range f_{low} to f_{high} , consisting of n_f frequency bins. x_i represents the measured SPL at the specified frequency bin while \bar{x} is the mean SPL of all frequencies at the measurement location under examination.

The second metric, average spatial variance, measures how much the frequency response of the room differs from point to point in the room. Spatial variance is calculated at each frequency bin for all measurement points and then the spatial variance values are averaged giving the average spatial variance of the room [12].

$$SV = \frac{1}{n_f} \sum_{i=f_{low}}^{f_{high}} \sqrt{\frac{1}{n_p - 1} \sum_{p=1}^{n_p} (x_{p,i} - \bar{x})^2} \quad (10)$$

Where the average spatial variance, SV , is calculated over all n_p listening points with $x_{p,i}$ representing the measured SPL at a specified point and frequency bin.

The following section will highlight the functionality and usefulness of this toolbox and provide verification of its accuracy.

5. SIMULATION EXAMPLES

This FDTD simulation toolbox is extremely flexible in allowing a number of different simulation options giving a user full control of room design, source signal/location, virtual measurement positions as well as

full analysis capabilities. This section will highlight these features.

5.1. Simulation Verification

Before working with complicated room/speaker setups, the simulation results must be verified. First, a simple three-dimensional rectangular room was set up to allow for direct comparison between expected room modes (from the room mode calculator function) and the simulated frequency response.

The room was set to dimensions of 5 x 4 x 3 meters with grid spacing of 10 cm in all directions and a 25 point measurement grid centered at (3.0 m, 2.0 m, 1.7 m). A single point source was placed near the corner of the room at (0.4 m, 0.4 m, 0.3 m). A 13th order MLS signal was used for the simulation with all walls set to have 10% absorption. Upon completion of the simulation, the measured frequency responses were plotted along with vertical lines overlaid at the expected modal frequencies (Figure 11).

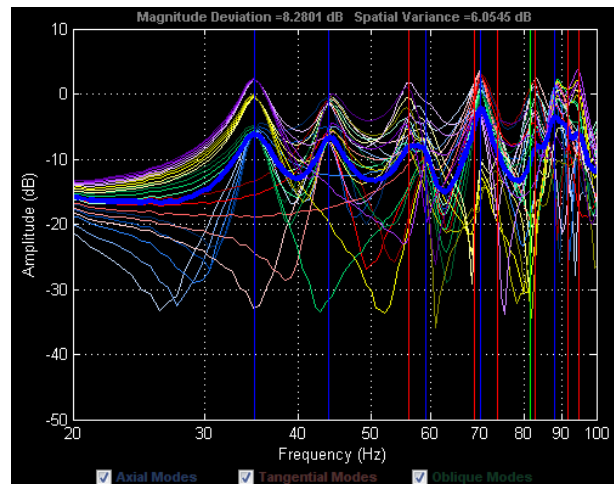


Figure 11: Comparison of measured frequency responses (heavy blue line = average response) to an MLS signal at the calculated expected modal values (blue = axial, red = tangential, green = oblique)

This comparison gives good indication that this simulation is providing accurate results since the expected modal values line up directly with the peaks of the average measured response of the room.

To give further verification, a number of simulations were run in the same room layout using sinusoidal signals set to single calculated modal frequencies. The

final SPL spatial distribution was then plotted and compared to the plots generated with the room mode calculator tool (Figures 12 – 14).

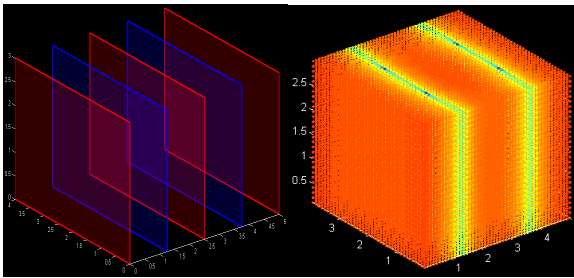


Figure 12: Axial mode (68.6 Hz) expected (left) and simulated (right) spatial distribution

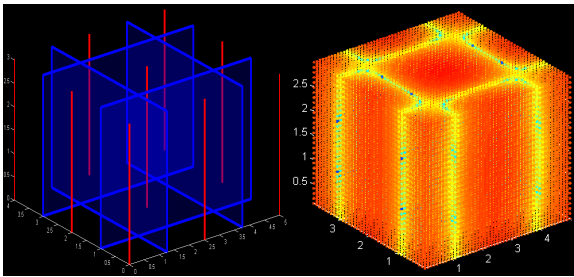


Figure 13: Tangential mode (109.8 Hz) expected (left) and simulated (right) spatial distribution

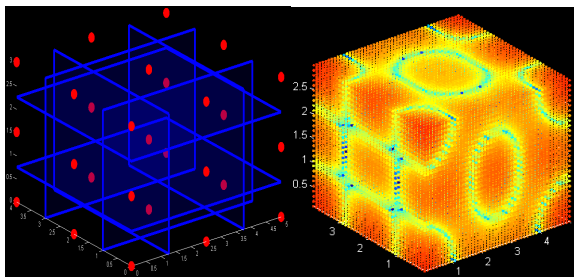


Figure 14: Oblique mode (158.5 Hz) expected (left) and simulated (right) spatial distribution

These comparisons further validate the simulation results. With this in mind, forward progress can be made using the toolbox with confidence that it provides accurate results.

5.2. Single subwoofer location

Subwoofer placement can have a massive effect on a room response. The majority of subwoofers commercially available have omnidirectional polar

patterns where the subwoofer operates as a pressure source. With this in mind, an omnidirectional subwoofer will cause a room to behave very differently depending on whether it is placed near a pressure node (pressure = minimum, particle velocity = maximum) or a pressure antinode (pressure = maximum, particle velocity = minimum). When placed at a node, the subwoofer will have very weak coupling with the room, causing the room mode to be minimally excited (Figure 15). The opposite is true when placement is near an antinode (Figure 16) [11].

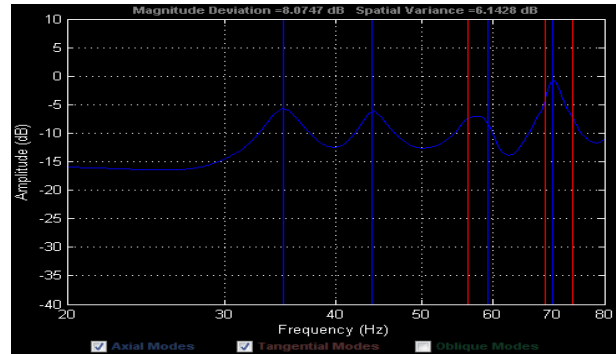


Figure 15: Average frequency response (25 measurement points) of a 5 x 4 x 3 m room with a single point source located at (0.2, 0.2, 0.2)

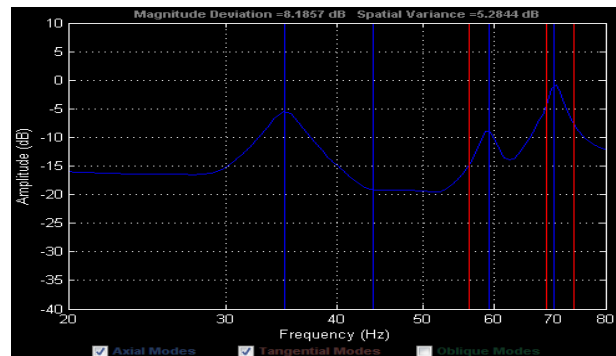


Figure 16: Average frequency response (25 measurement points) of a 5 x 4 x 3 m room with a single point source located at (0.2, 2.0, 0.2)

The suppressed mode in Figure 16 corresponds to the (0, 1, 0) axial mode expected to occur at 42.875 Hz. Using the room mode calculator again to access the two source locations tested (Figure 17), it is clear that the first location (0.2, 0.2, 0.2) is very close to an antinodal plane for 42.875 Hz, while the second location (0.2, 2.0, 0.2) is directly on a nodal plane. As expected, the first

location strongly excites the room mode while the second location hardly excites the mode at all.

With this concept in mind, it would be expected that placing the source directly in the center of the room would greatly suppress many low order axial modes that have antinodal points/planes at the center (Figure 18).

The low order modes of (1, 0, 0), (0, 1, 0), (0, 0, 1) and (1, 1, 0) all have been minimally excited due to the source's central placement.

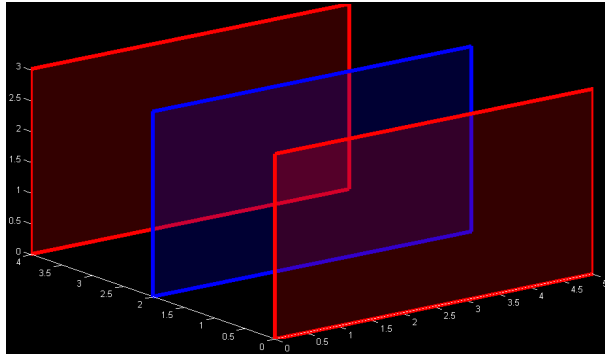


Figure 17: Expected spatial distribution of (0, 1, 0) mode occurring at 42.875 Hz

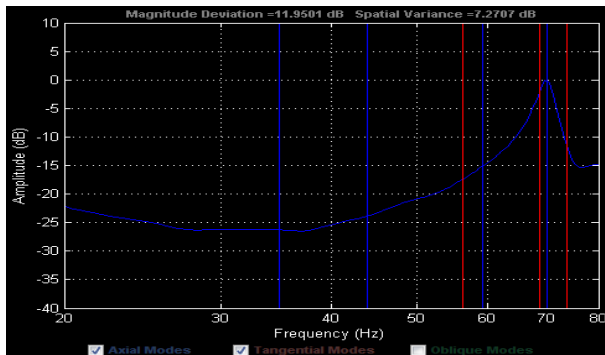


Figure 18: Average frequency response (25 measurement points) of a 5 x 4 x 3 m room with a single point source located at (2.5, 2.0, 1.5)

5.3. Multiple subwoofers

More often than not, subwoofer placement is restricted by reality (often by obstacles present in the room). In most cases, placement of a single subwoofer in the center of the room to best reduce the lower order modes is not possible. This problem can be addressed by utilizing a multiple subwoofer system.

The key to this technique is placing the subwoofers at antinodal positions of opposite polarity [11]. That is, one subwoofer is at a positive pressure amplitude maximum while the other is at a negative pressure amplitude maximum. This placement will cause acoustical cancellation of the room mode and give similar results to placing a single subwoofer at that mode's node (Figure 19).

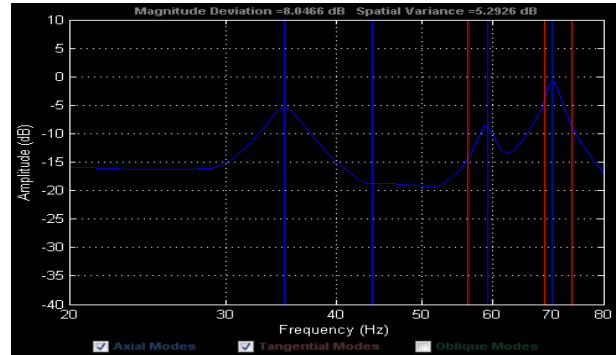


Figure 19: Average frequency response (25 measurement points) of a 5 x 4 x 3 m room with two point sources located at (0.2, 2.0, 0.2) and (0.2, 3.8, 0.2)

The plot in Figure 19 is nearly identical to that in Figure 16, which utilized the single subwoofer placed at a node to achieve modal suppression.

Having achieved suppression of the first-order mode along the length of the room, two more subwoofers can be placed at the other corners to help suppress the first-order mode along the width of the room (Figure 20).

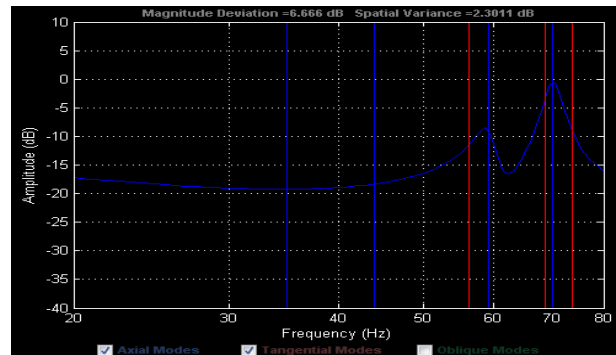


Figure 20: Average frequency response (25 measurement points) of a 5 x 4 x 3 m room with four point sources located at (0.2, 0.2, 0.2), (0.2, 3.8, 0.2), (4.8, 0.2, 0.2) and (4.8, 3.8, 0.2)

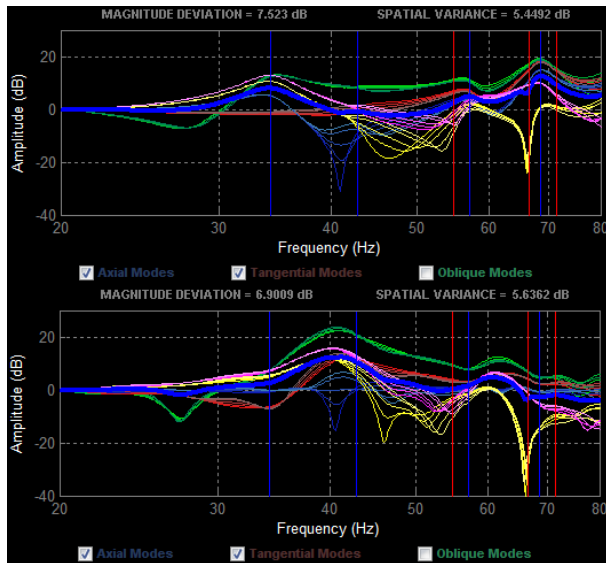


Figure 21: Average frequency response (25 measurement points) of a 5 x 4 x 3 m room with one point source at (0.2, 2.0, 0.2) with no equalization (top) and single-point equalization (bottom)

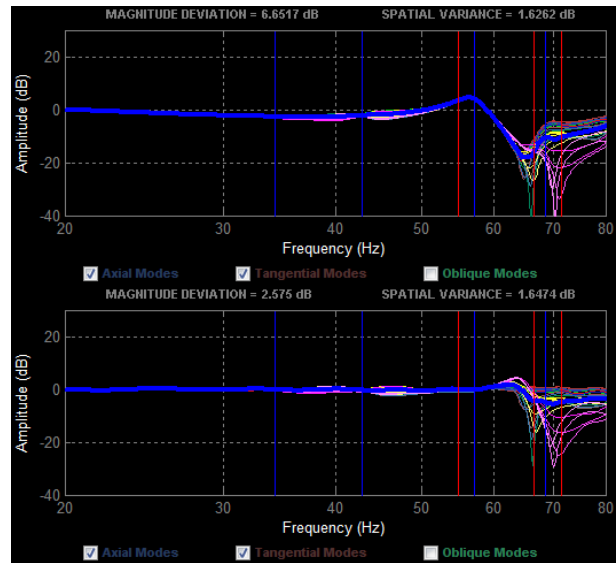


Figure 22: Average frequency response (25 measurement points) of a 5 x 4 x 3 m room with four point sources at (0.2, 2.0, 0.2), (4.8, 2.0, 0.2), (2.5, 0.2, 0.2) and (2.5, 3.8, 0.2) with no equalization (top) and single-point equalization (bottom)

The advantage of a multiple subwoofer system is the significant decrease in spatial variance between listening points. While using a single subwoofer, global equalization may help to flatten the response at certain locations, but will cause other locations to become worse (Figure 21).

With a properly configured multiple subwoofer system, the listening locations all follow a very similar response allowing effective global equalization to be applied to the system with all points benefiting (Figure 22).

In both cases above, the spatial variance does not improve due to the single point equalization. In fact, with the single subwoofer configuration, the spatial variance becomes worse with single-point equalization. Magnitude deviation, on the other hand, is greatly reduced with the multiple subwoofer system by over 4 dB. This means that, on average, the listening locations experience an overall flat response with single-point equalization. Listeners in a room with this system would generally have similar listening experiences due to low magnitude deviation and spatial variance.

5.4. Polar pattern control

Another helpful feature of the FDTD simulation toolbox is the ability to experiment with polar pattern control of a source. Currently, this is limited to positioning and delaying a number of point sources, but still allows for helpful illustrations of how polar patterns can be controlled.

In one example, two point sources are placed in an anechoic environment 20 cm apart, with one source having reversed polarity. When driven by a sinusoidal signal, a clear dipole pattern emerges (Figure 23).

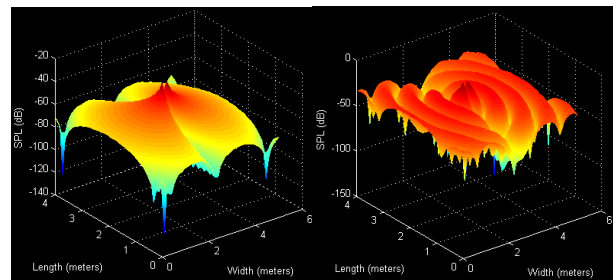


Figure 23: Simulated polar pattern with two point sources separated by 20 cm and opposite polarities (left = 30 Hz, right = 250 Hz)

By adding a 0.5 ms delay to one of the sources, this dipole pattern now shifts to become more of a cardioid shape (Figure 24).

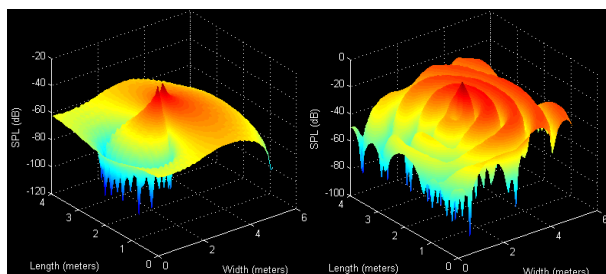


Figure 24: Simulated polar pattern with two point sources separated by 20 cm, 0.5 ms delay and opposite polarities (left = 30 Hz, right = 250 Hz)

An additional analysis option within the toolbox is to examine the diffraction caused by loudspeaker enclosures. This is accomplished by creating obstacles within a room that intersect to create a box. A point source is then positioned at a small opening on one side to approximate a drive unit. A simple example is given in Figure 25 with a sealed enclosure driven at various frequencies.

It is possible to examine a non-rectangular enclosure configuration, such as an elliptical design (Figure 26). This can help examine whether a special enclosure design will reduce diffraction, giving a more even polar pattern. The example highlighted in Figure 26 shows a significant decrease in diffraction at both 250 Hz and 800 Hz due to the rounded shape of the enclosure.

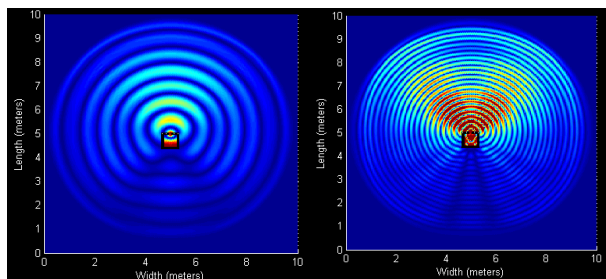


Figure 25: Simulated polar pattern of a simple sealed enclosure (left = 250 Hz, right = 800 Hz)

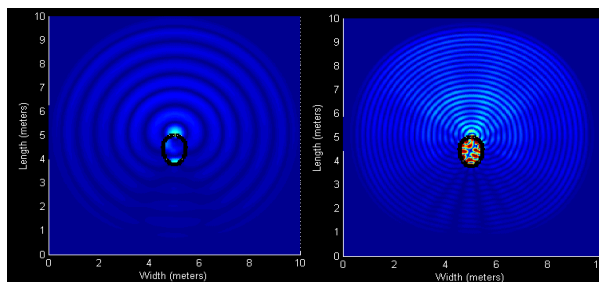


Figure 26: Simulated polar pattern of an elliptical sealed enclosure (left = 250 Hz, right = 800 Hz)

5.5. Non-rectangular spaces

A central feature of the toolbox is the ability to model non-rectangular spaces in either two or three dimensions. This allows for much more realistic simulations of real-world conditions.

One common spatial configuration is an L-shaped room, where two separate rooms of a house are often connected. Such an example is displayed in Figure 27 in a 2D and 3D configuration. Note that pressure maxima still occur at corners, so the subwoofer placement techniques highlighted in Sections 5.2 and 5.3 are still valid.

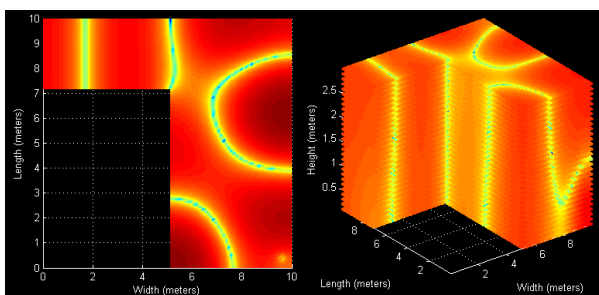


Figure 27: Simulation of a 2D (left) and 3D (right) L-shaped room with a single source located at (9.5, 0.5, 0.5) and driven by a 50 Hz sinusoidal signal

Any shape, beyond a simple L-shaped room is also possible with this simulation technique such as a triangular wedge (Figure 28), a domed structure (Figure 29) or a sphere (Figure 30). Obstacles can be placed within the room (Figure 31) and also a complex of rooms can be modeled with hallways connecting them (Figure 32).

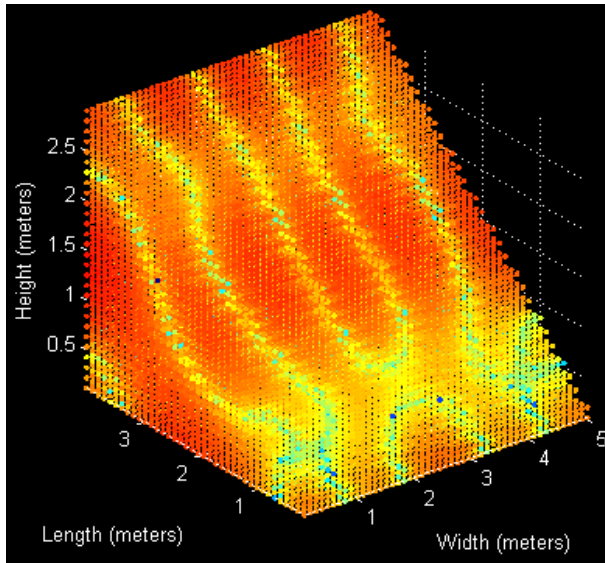


Figure 28: Simulation of a triangular wedge excited by a single source located at (2.5, 3.5, 0.5) driven by a 200 Hz sinusoidal signal

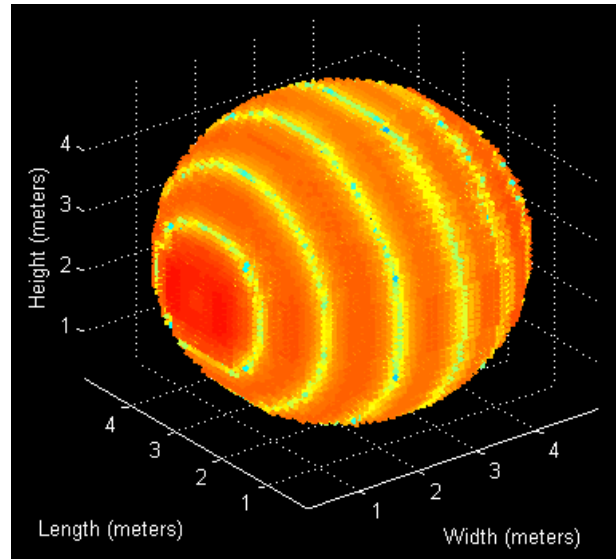


Figure 30: Simulation of a spherical room excited by a single source located at (0.5, 2.5, 2.5) driven by a 200 Hz sinusoidal signal

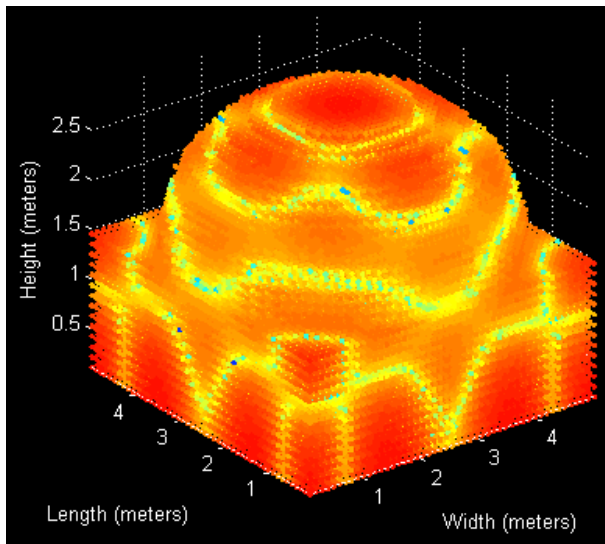


Figure 29: Simulation of a domed structure excited by a single source located at (2.5, 2.5, 0.5) driven by a 200 Hz sinusoidal signal

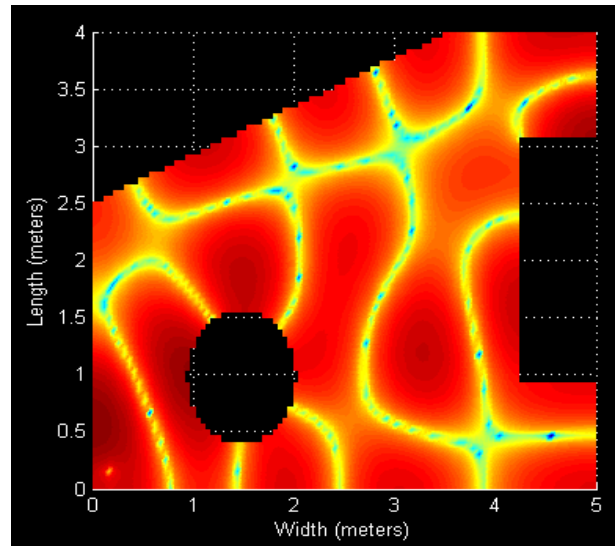


Figure 31: Simulation of a 2D non-rectangular room with obstacles excited by a single source located at (0.2, 0.2) driven by a 200 Hz sinusoidal signal

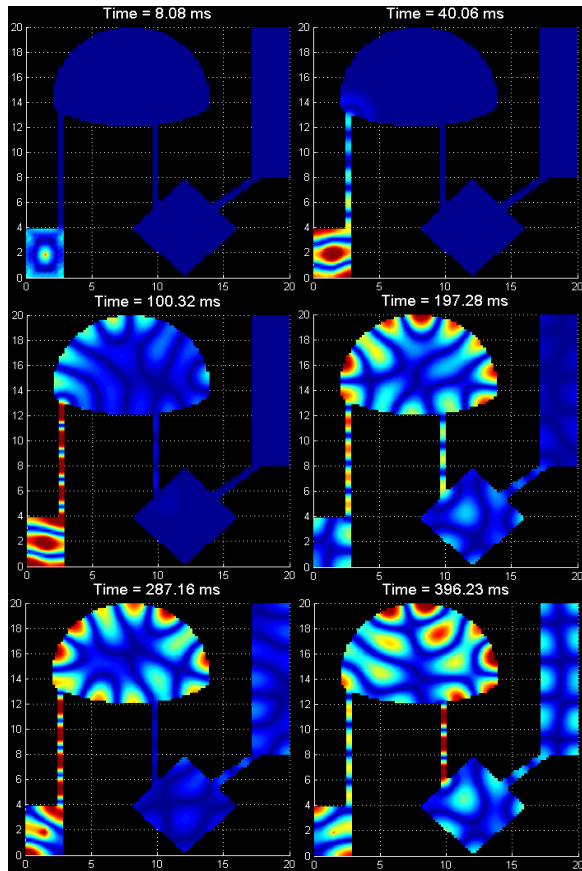


Figure 32: Simulation of a 20 m x 20 m 2D complex of rooms excited by a single source located at (1.5, 2.0) driven by an 80 Hz sinusoidal signal (at various stages of the simulation)

6. CONCLUSIONS

An acoustics simulation toolbox has been presented that utilizes the low-frequency accuracy of the FDTD method. The toolbox can handle simulation of any two- or three-dimensional spatial configuration with very flexible parameters controlling the source(s), virtual measurements and analysis.

A key feature is the ability to visualize a sound wave propagating through a space over time. This allows for close examination of room mode spatial distribution and interaction (if any) between the sound waves and any room obstacles.

Along with the analysis options, this can allow for proper design and configuration of a listening space and subwoofer system with the ability to inspect the layout

in a virtual environment before committing to anything in the real-world.

Future development of this toolbox will focus on an automatic adaptive equalization technique based on the FDTD simulation. This will be aimed to give beneficial low frequency equalization throughout a listening area, based on the measurement locations in the FDTD simulation.

In addition to the equalization procedure development, efforts will be made to expand the currently simple auralization function in the toolbox to give a useful technique for virtual evaluation of a room response using headphones. Currently, the auralization procedure involves running an audio signal through a simple two-way crossover and using the low-frequency component in the FDTD simulation. The high-frequency component is simply delayed to match the propagation delay in the room simulation.

This software has not been developed to become a commercial product. It has been created to serve as a powerful tool for the authors' ongoing research into low-frequency control.

7. REFERENCES

- [1] CATT-Acoustic, www.catt.se
- [2] Odeon Room Acoustics Software, www.odeon.dk
- [3] LMS RAYNOISE, www.lmsintl.com
- [4] Olesen, Soren Krarup. "Low frequency room simulation using finite difference equations." AES Convention #102, Preprint 4422. March 1997.
- [5] Suzuki, Hisaharu. "Treatment of boundary conditions by FDTD method." Acoustics, Science and Technology. Volume 28. 2007.
- [6] Celestinos, Adrian; Sofus Birkedal Nielsen. "Multi-source low frequency room simulation using finite difference time domain approximations." Audio Engineering Convention #117, Preprint 6264. October, 2004.
- [7] Celestinos, Adrian; Sofus Birkedal Nielsen. "Low frequency room simulation using FDTD." JAES Volume 56 Issue 10. October, 2008.

- [8] Kowalczyk, Konrad; Maarten Van Walstijn. "Modeling frequency dependent boundaries as digital impedance filters in FDTD and K-DWM Room Acoustics Simulations." JAES Volume 56 Issue 7/8. July/August 2008.
- [9] Tolan, Julius G; John B. Schneider. "Locally conformal method for acoustic finite- difference time-domain modelling of rigid surfaces." 140th Meeting of the Acoustical Society of America. July 27, 2003.
- [10] Welti, Todd; Allan Devantier. "Low frequency optimization using multiple subwoofers." JAES Volume 54 Issue 5. May, 2006.
- [11] Toole, Floyd E. *Sound Reproduction: Loudspeakers and Rooms*. Focal Press, New York. 2008.
- [12] Celestinos, Adrian; Sofus Birkedal Nielson. "Optimizing placement and equalization of multiple low frequency loudspeakers in rooms." AES Convention #119, Preprint 6545. October, 2005.